

Reply to the referees' review of:

## **On the sensitivity of aerosol-cloud interactions to changes in sea surface temperature in radiative-convective equilibrium**

Reviewer #1

We would like to thank Reviewer #1 for his constructive suggestions. Please find below a point-by-point reply to all the referee's comments (in blue).

Lorian and Dagan, 2023 uses idealized simulations in radiative-convective equilibrium to study the effects of changing aerosol concentrations on radiation and precipitation at different sea surface temperatures. The authors find that while the effects on radiation are qualitatively similar at all temperatures, the effect decreases with increasing SST. The manuscript attributes the decrease in SST-mediated changes in aerosol-cloud interaction to differential aerosol effects on warm rain formation and cloud liquid in lower parts of deep convective clouds. These become deeper at higher SSTs, leading to different responses. Another interesting result I want to highlight here is the anvil cloud fraction and ice water path decrease with increasing aerosol number, that is caused by increased latent heating and consequently increased upper tropospheric stability, following the "stability iris" hypothesis.

This manuscript presents several novel results on a very important and understudied topic. However, I am not convinced about some of the proposed explanations. In particular, I remain skeptical about the radiative relevance of changes in the warm parts of deep convective clouds. Can these really modify changes in radiative fluxes at the top of the atmosphere, given that they lie below very reflective thick anvil clouds? Furthermore, my main suggestion to the authors would be to go beyond the domain-average perspective and try to decompose changes in different cloud types (for example active deep convective cores, thick anvils, thin anvils, low clouds).

Overall, I found the manuscript to be an interesting read, full of noteworthy insights. However, I would strongly encourage that the authors to consider further clarification or even revision of some of their key findings to improve the overall quality of their work prior to final publication. For a more detailed discussion, please see my extended comments below.

### **General comments:**

We reply to the next two comments together as they are strongly connected.

1. Regions dominated by deep convective lifecycle that are at/near conditions of radiative-convective equilibrium are typically dominated by anvil clouds, both in terms of coverage as well as radiative impact (e.g. Berry and Mace, 2014). The radiative importance of deep convective cores is, despite their strong LW and SW radiative effects, relatively small due to their small coverage. Changes in their properties/frequency are therefore unlikely to substantially modify climatological CRE. Moreover, given the large IWP of deep convective cores (see e.g. Fig. 1 in Sokol and Hartmann, 2020), I find it hard to believe that changes in the warm parts of deep convective clouds can directly influence TOA radiation. Couldn't changes in TOA radiative fluxes be entirely related to changes in anvil clouds?
2. On the other hand, even in disaggregated RCE simulations, there is a small but non-negligible population of stratiform low clouds as shown in Figure 1a. What fraction of changes in cloud liquid, rain, and their radiative implications can be attributed to changes in stratiform liquid clouds?

→As mentioned above, it is difficult to answer my two key questions without digging deeper into the model output, beyond the domain averages. My first thought would be to perform an analysis of the 2D SAM model output fields and subdivide the domain into, for example, areas of active deep convection, thick anvils, thin anvils, and low clouds. This could be done, for example, based on the diagnosed ice water path fields. In addition, it may be useful to look at changes in COD/in-cloud CRE to distinguish between effects on cloud fraction and cloud opacity.

**Reply:** Many thanks for raising this important point and for the nice suggestion to examine the response by cloud type. Following this comment significant modifications were implemented into the revised manuscript as elaborated below.

For examining the different cloud types, in the revised manuscript we are presenting 2D histograms of liquid water path ( $\mathcal{L}$ ) and ice water path ( $\mathcal{I}$ ) and the response of these cloud types to changes in  $N_a$ . The figure below, which was added to the revised manuscript as Fig. 4, presents the 2D histograms of the cloud fraction (CF) at the different bins of  $\mathcal{L}$  and  $\mathcal{I}$  and the average total, shortwave and longwave cloud radiative effect (CRE) at these different bins. These quantities are presented for two simulations using the lowest ( $20 \text{ cm}^{-3}$ ; panels a-d) and the highest ( $2000 \text{ cm}^{-3}$ ; panels e-h)  $N_a$  and SST = 290 K. In addition, the difference between the high and low  $N_a$  conditions is presented in panels i-l. As the reviewer mentioned, this figure illustrates that the CF in these RCE simulations is dominated by anvil clouds (e.g. Wing et al., 2020), i.e., clouds with negligible  $\mathcal{L}$  and high (thick anvil clouds; denoted by marker 1 in Fig. 4a) or low (thin anvil clouds; denoted by marker 2 in Fig. 4a)  $\mathcal{I}$ . However, this figure also demonstrates the existence of two+ other types of clouds in these RCE simulations - shallow clouds (high  $\mathcal{L}$  and low  $\mathcal{I}$ ; denoted by marker 3 in Fig. 4a) and deep convective cores (high  $\mathcal{L}$  and high  $\mathcal{I}$ ; denoted by marker 4 in Fig. 4a). Examining the difference between the high and low  $N_a$  simulations demonstrates that an increase in  $N_a$  drives a thinning of the anvil clouds, i.e., an increase in the frequency of thin anvil clouds and a decrease in the frequency of thick anvil clouds (Fig. 4i). It also demonstrates that with the increase in  $N_a$  the CRE becomes more negative for all  $\mathcal{L}$  and  $\mathcal{I}$  (and especially for low  $\mathcal{I}$  and medium-high  $\mathcal{L}$ ; Fig. 4j) bins, driven mostly by changes in the SW (Fig. 4k), which are driven by the Twomey effect (Twomey, 1977), with only a minor change in the LW (Fig. 4l). This interesting trend is now presented and discussed in the revised manuscript, which we believe improved the contribution of our paper.

In addition to the continuum/histogram perspective presented in Fig. 4, we examine the relative change in the total ice CF ( $CF_{ice}$ ) with  $N_a$ , which is calculated by integrating over thick ice plus thin ice regimes as defined in Table S1, SI (see below; see also Sokol et al., 2024). This calculation demonstrates that, as was reported in the original manuscript, the  $CF_{ice}$  is reduced with an increase in  $N_a$  for all SSTs examined here (Fig. 5a). In addition to the changes in the  $CF_{ice}$ , as the reviewer suggests, there is a non-negligible shallow cloud fraction ( $CF_{shallow}$ , calculated as the integral over the shallow clouds regime as defined in Table S1, SI) in the domain, which affects the SW (Fig. 4c). These shallow clouds become more reflective in the SW with an increase in  $N_a$  due to the Twomey

effect (Fig. 4k), and their fraction also changes in a way that depends on the SST (Fig. 5b).

Specifically, Fig. 5b demonstrates that  $CF_{shallow}$  increases with  $N_a$  under low SSTs and decreases with  $N_a$  under high SST. This trend can help understand the higher SW sensitivity to  $N_a$  under low SSTs compared with high SST, as under high SST the Twomey and the  $CF_{shallow}$  effects counteract each other while under low SSTs they add to each other. Please see more details about this decomposition below.

In addition, following the reviewer's suggestion, we are decomposing the radiative response to contributions from changes in CF and from changes in cloud optical depth. This is done by a linear decomposition following Bony (2004) and Sokol (2024). This analysis demonstrates that the net radiative response is coming from changes in both ice and shallow clouds. Please see the details below.

The additions to the revised manuscript:

*“Figs. 1, 2, 3 examine the bulk cloud and radiative properties in the domain. However, as previously demonstrated, the impact of aerosols on clouds is cloud regime dependent (Gryspeerd and Stier, 2012; Christensen et al., 2016; Dagan and Stier, 2020b). Therefore, it is crucial to analyze the distribution of cloud regimes in our simulations and discern how each specific cloud regime responds to the increase in  $N_a$ . In this paper we define the cloud regimes based on different bins of  $\mathcal{L}$  and  $\mathcal{I}$ . For that purpose, Fig. 4 presents 2D histograms of the cloud fraction (CF), or cloud occurrence, at the different bins of  $\mathcal{L}$  and  $\mathcal{I}$  and the average total, shortwave and longwave CRE at these different bins, all for the coldest case considered here (SST = 290 K) as an example. This figure illustrates that the CF in these RCE simulations is mostly dominated by anvil clouds (e.g. Wing et al., 2020), i.e., clouds with negligible  $\mathcal{L}$  and high (thick anvil clouds; denoted by marker 1 in Fig. 4a) or low (thin anvil clouds; denoted by marker 2 in Fig. 4a)  $\mathcal{I}$ . We note that the average CRE of thin anvil cloud is small but not positive as in previous assessments (Sokol, 2024), probably due to the use of a relatively coarse resolution of  $\mathcal{L}$  and  $\mathcal{I}$  bins. However, Fig. 4a also illustrates the existence of two other types of clouds in these RCE simulations - shallow clouds (high  $\mathcal{L}$  and low  $\mathcal{I}$ ; denoted by marker 3 in Fig. 4a) and deep convective cores (high  $\mathcal{L}$  and high  $\mathcal{I}$ ; denoted by marker 4 in Fig. 4a). In addition, Fig. 4 i-l illustrates the difference between simulations with the highest ( $2000 \text{ cm}^{-3}$ ) and the lowest ( $20 \text{ cm}^{-3}$ )  $N_a$  conditions. Specifically, Fig. 4i illustrates that an increase in  $N_a$  drives thinning of the anvil clouds, i.e., an increase in the frequency of thin anvil clouds and a decrease in the frequency of thick anvil clouds. Furthermore, Fig. 4 j-l illustrate that with an increase in  $N_a$  the CRE decreases for all  $\mathcal{L}$  and  $\mathcal{I}$  bins (and especially for medium-high  $\mathcal{L}$*

and low  $\mathcal{I}$ ; Fig. 4j), driven mostly by changes in the SW (Fig. 4k), with only minor changes in the LW (Fig. 4l). This SW difference with  $N_a$  can be explained by the Twomey effect (Twomey, 1974). Following the method outlined in (Sokol, 2024), we calculate the total ice cloud fraction ( $CF_{ice}$ ) as the integral over thick ice plus thin ice regimes as defined in Table S1, SI. Fig. 5a illustrates a (mostly) monotonic decrease across SSTs in  $CF_{ice}$  with increasing  $N_a$ , consistent with the domain mean CF reduction (Fig. 2c). We note that not just the integrated  $CF_{ice}$  decreases with  $N_a$ , but the entire distribution of  $\mathcal{I}$  is shifted to lower values (i.e., thinning of the anvil clouds; Figs. 4i, 2b and 3h). A decrease in  $CF_{ice}$  leads to more outgoing LW radiation out of the atmosphere and reduces  $\Delta R^{LW}$ , as can be seen in Fig. 1b. In addition, Fig. 5b presents the relative change in the shallow cloud fraction ( $CF_{shallow}$ ; calculated as the integral over the shallow regime as defined in Table S1, SI). We note that this definition of shallow clouds might also include two-layer cloud conditions with cirrus clouds with relatively low  $\mathcal{I}$  above shallow clouds. Figure 5b illustrates a rise in  $CF_{shallow}$  with  $N_a$  for low SST, while for high SST it illustrates a decrease in  $CF_{shallow}$  with  $N_a$  (the change in the shallow cloud fraction is not observed in Fig. 4i due to the dominance of ice clouds, which inflates the color-bar range). We note that although the relative changes in  $CF_{ice}$  and  $CF_{shallow}$  has similar magnitudes, the baseline (i.e., referring to the simulated value, and not the difference between the most polluted and cleanest runs)  $CF_{ice}$  is two orders of magnitude larger than  $CF_{shallow}$  (Fig. S6, SI).

Fig. 4 illustrates that the response of the CRE to an increase in  $N_a$  is driven both by changes in CF (Fig. 4i) and by changes in CRE for a given bin of  $\mathcal{L}$  and  $\mathcal{I}$  (Fig. 4j). Next, we aim to quantitatively separate these two effects. Thus, we write the total CRE as the integral over the different bins of  $\mathcal{L}$  and  $\mathcal{I}$  of the CF times the CRE in each bin:

$$CRE = \int_0^{\infty} \int_0^{\infty} CRE(\mathcal{L}, \mathcal{I}) CF(\mathcal{L}, \mathcal{I}) d\mathcal{L}d\mathcal{I}$$

In the simulations presented here  $\Delta CRE \approx \Delta R$  (Fig. 1). Thus, following a somewhat similar method to that presented in Bony, 2004 and Sokol, 2024, we decompose the mean  $\Delta R$  into three contributions: a) changes in  $\Delta R$  due to changes in the cloud's opacity per  $\mathcal{L}$  and  $\mathcal{I}$  bin (the opacity term or the Twomey term), (b) a shift in the occurrence or CF in each  $\mathcal{L}$  and  $\mathcal{I}$  bin (the shift term or the  $\mathcal{L}/\mathcal{I}$  term), and (c) the combined effect of changes in the cloud's opacity and shift (the nonlinear term). Mathematically, this decomposition can be written as:

$$\begin{aligned}
\Delta CRE &\approx \Delta R \\
&= \underbrace{\int_0^\infty \int_0^\infty \Delta CRE(\mathcal{L}, \mathcal{I}) CF(\mathcal{L}, \mathcal{I}) d\mathcal{L} d\mathcal{I}}_{\text{Opacity}} \\
&+ \underbrace{\int_0^\infty \int_0^\infty CRE(\mathcal{L}, \mathcal{I}) \Delta CF(\mathcal{L}, \mathcal{I}) d\mathcal{L} d\mathcal{I}}_{\text{Shift}} \\
&+ \underbrace{\int_0^\infty \int_0^\infty \Delta CRE(\mathcal{L}, \mathcal{I}) \Delta CF(\mathcal{L}, \mathcal{I}) d\mathcal{L} d\mathcal{I}}_{\text{nonlinear}}
\end{aligned}$$

The opacity term represents changes in the CRE while the CF and  $\mathcal{L}/\mathcal{I}$  distribution are held fixed, i.e., multiplying Fig. 4a with Fig. 4j, while the shift term represents changes in the CF while the CRE per  $\mathcal{L}$  and  $\mathcal{I}$  bin is held fixed, i.e., multiplying Fig. 4b with Fig. 4i. Lastly, the nonlinear term is acquired, for example, by multiplying Fig. 4i with Fig. 4j.

Fig. 6a-c illustrates the decomposition presented in eq. 5 for the domain mean (i.e., integrating over all  $\mathcal{L}$  and  $\mathcal{I}$  bins excluding the no clouds regime as defined in Table S1, S1) for all the different SSTs. Fig. 6a-c also present the simulated response as presented in Fig. 1 (referred to as "Model") and the sum over the three terms presented in eq. 5 (referred to as "Total"). These panels illustrate that the opacity term is the main driver for the decline in  $\Delta R$  with  $N_a$  (Fig. 6a), occurring mostly through the SW (Fig. 6b). In addition, this figure illustrates that the opacity term is the main driver for the SST-sensitivity, demonstrating a generally weaker response as the SST increases, consistent with Fig. 1. The shift term, on the other hand, demonstrates similar magnitudes but opposite sign in the SW and LW (Figs. 6b and c, respectively), with a weak SST-dependence, thus making this term negligible in the total (Fig. 6a). The nonlinear term shows close to zero contributions to  $\Delta R$  and its SW and LW components, thus justifying focusing on the linear decomposition in eq. 5. We note that the decomposition results in a similar magnitude and SST-trend as the model (comparing Total to Model in Fig. 6a-c), thus justifying its use. However, we also note a slight over-estimation of  $\Delta R$  using the decomposition at the lower SSTs (Fig. 6a).

In addition to the domain mean,  $\Delta R$  is decomposed per cloud regime by integrating over the relevant part of the  $\mathcal{L}$  and  $\mathcal{I}$  phase-space (Fig. 6d-f and Table S1, SI). These panels illustrate that deep convective cores have negligible contributions to  $\Delta R$ ,  $\Delta R^{SW}$  and  $\Delta R^{LW}$ , mostly due to their small coverage (Fig. 4a). Therefore, most of the contribution to  $\Delta R$  comes from anvil and shallow clouds changes.

The thick and thin ice clouds' response drives a negative net total  $\Delta R$ , which is stronger under lower SSTs (Fig. 6d). This trend is dominated by the opacity term, which is driven almost entirely by the SW part of the spectrum (Fig. 6e). This term represents an increase in the reflectivity of the ice clouds for a given  $\mathcal{L}$  and  $\mathcal{I}$  distribution, and can be explained by a similar mechanism to the Twomey effect but for ice particles. This term becomes stronger (more negative) with a reduction in SST due to an increase in the baseline CF of these clouds (Fig. S6, SI). The shift term in thick ice clouds is strongly positive in the SW (Fig. 6e) and negative in the LW (Fig. 6f) due to the thinning of the ice clouds and the general reduction of the occurrence of these thick clouds (4i). However, the net effect of the shift term is low, for both thick and thin ice clouds, due to cancellation between the SW and the LW (Fig. 6d).

Similarly to the ice clouds' response, the shallow clouds' response also drives a negative net total  $\Delta R$ , which becomes stronger under lower SSTs (Fig. 6d). As expected, changes in shallow clouds have a small impact in the LW (Fig. 6f), but a significant effect in the SW (Fig. 6e). As in ice clouds, the negative net total  $\Delta R$  in the shallow clouds case is driven mostly by the opacity term, which in this case can be explained by the classical Twomey effect. Here again, the opacity term demonstrates a sensitivity to the underlying SST, and becomes stronger for lower SST due to an increase in the baseline CF (Fig. S6, SI). However, we note that the opacity term's SST-sensitivity cannot solely explain the SST-sensitivity in the total effect of shallow clouds (Fig. 6d). The shallow clouds' shift term also contributes to the total SST-sensitivity. This term, while having a relatively small magnitude, is negative under low SSTs and positive under high SSTs, consistent with the relative change in  $CF_{shallow}$ , which is positive under low SSTs and negative under high SSTs (Fig. 5b). The contrasting response of  $CF_{shallow}$  to  $N_a$  under the different SSTs can be explained by warm rain suppression at varying depths of warm layers. As was noted above, with an increase in SST, the freezing level increases, while an increase in  $N_a$  acts to push warm rain formation to higher levels (Rosenfeld, 2000; Freud and Rosenfeld, 2012; Heikenfeld et al., 2019). Thus, under lower SSTs, for which the freezing level is relatively shallow, an increase in  $N_a$  can suppress warm rain (see Fig. 3g) and hence lead to an increase in  $CF_{shallow}$ . In contrast, under higher SSTs, for which the

freezing level is relatively deep, an increase in  $N_a$  drives warm rain suppression at the lower levels, which is compensated for at higher levels of the warm section (Fig. 3g), thus eliminating the positive effect on  $CF_{shallow}$ .

The combined response of ice and shallow clouds to an increase in  $N_a$ , as explained in this section, can explain the reduction in  $\Delta R^{LW}$  with  $N_a$ , the reduction in  $\Delta R^{SW}$  with  $N_a$  and its SST-sensitivity, and hence the reduction in  $\Delta R$  with  $N_a$  and its SST-sensitivity (Fig. 1).”

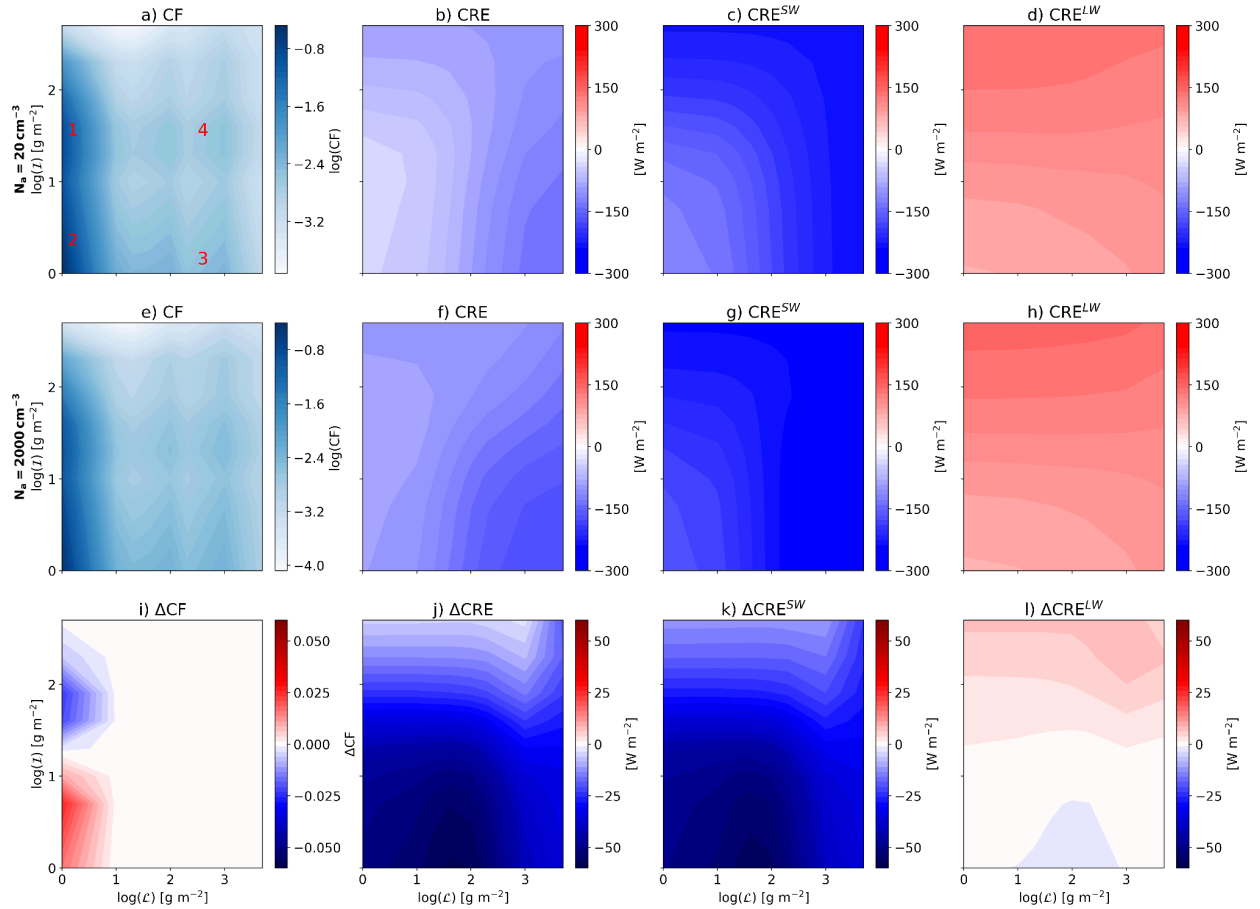


**Figure 4.** Domain and time mean two-dimensional histograms of cloud fraction (CF; **a** and **e**), at different bins of liquid water path ( $\mathcal{L}$ ) and ice water path ( $\mathcal{I}$ ) and the average total (**b** and **f**), shortwave (**c** and **g**) and longwave (**d** and **h**) cloud radiative effect (CRE) at these different bins. These quantities are presented for two simulations using the lowest ( $N_a = 20 \text{ cm}^{-3}$ ; **a-d**), and the highest ( $N_a = 2000 \text{ cm}^{-3}$ ; **e-h**)  $N_a$ , under SST = 290 K. In addition, the difference between the highest and lowest  $N_a$  conditions is presented in panels **i-l**.



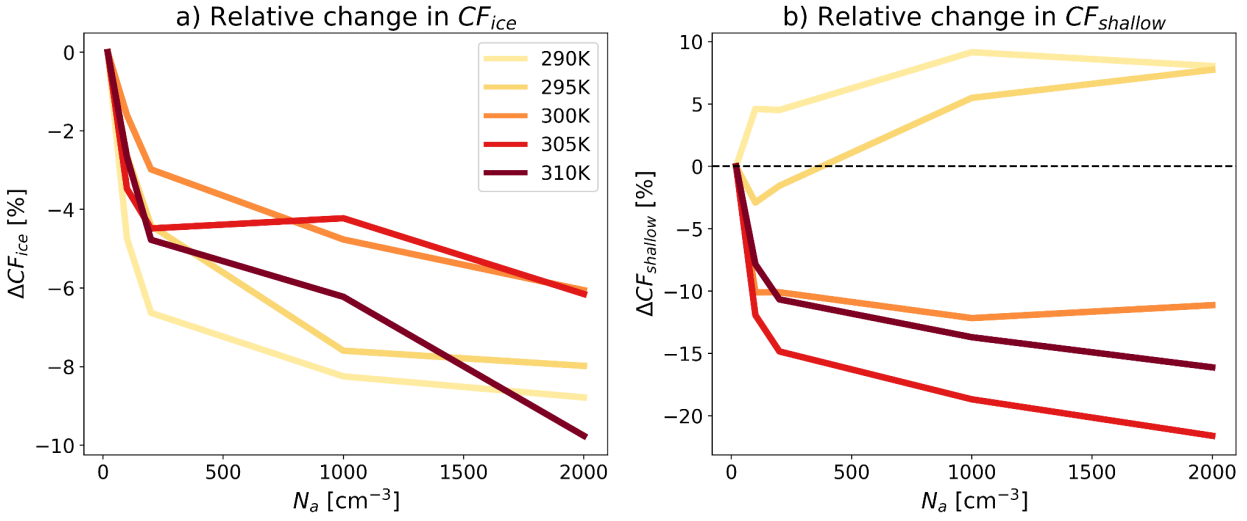


**Figure 5.** The relative response of domain and time mean ice cloud fraction ( $CF_{ice}$ ; **a**) and shallow cloud fraction ( $CF_{shallow}$ ; **b**) to an increase in  $N_a$ . The values are shown as a difference, relative to the cleanest run (as denoted by the  $\Delta$  sign), for each SST. The baseline  $CF_{ice}$  and  $CF_{shallow}$  are presented in Fig. S6, SI.

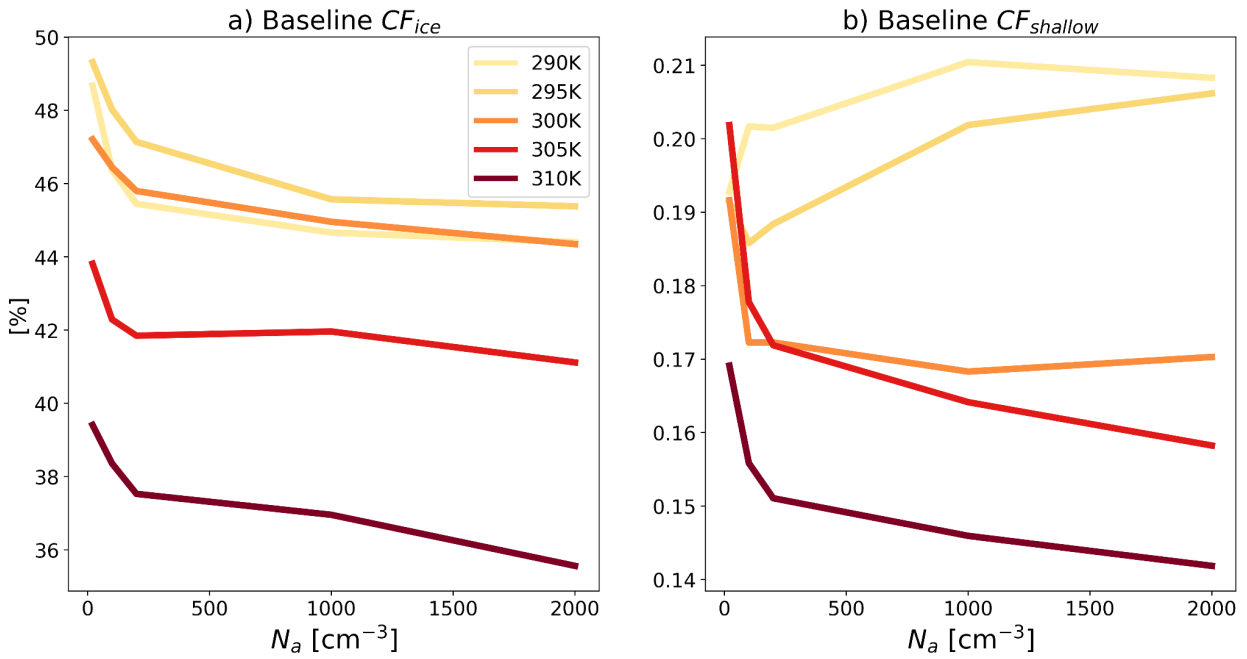


**Figure S6.** Changes in domain and time mean cloud fraction with  $N_a$  for ice clouds ( $CF_{ice}$ ; **a**) and shallow clouds ( $CF_{shallow}$ ; **b**), for each SST.

1. Figures 3a and 6h make me wonder if the effect of aerosols on clouds also affects cloud height, cloud top temperature, and thus the radiative budget. High aerosol simulations seem to lead to higher, colder clouds. This may be a radiatively important mechanism that should be discussed. Is the decrease in cloud top temperature strong enough to significantly affect the LW CRE?

**Reply:** Thank you for raising this important question. Following this comment we examine the sensitivity of the cloud top temperature and height to  $N_a$ . For doing that, we define the domain-mean cloud top to be at the level for which the domain-mean total condensed water crosses an arbitrary threshold. Three different thresholds were used ( $0.5, 1, 2 \cdot 10^{-3}$  [g kg<sup>-1</sup>]) in order to check if the results are threshold dependent. For each SST, we used the cleanest run ( $N_a = 20$  cm<sup>-3</sup>) as a reference. As can be seen in the figure below (Fig. R1), cloud top height changes with aerosols are non-monotonic, non SST- and threshold-consistent and small (relative to the vertical resolution, i.e., the difference is only one grid point to each direction - Fig. R1b, d and f), for all three thresholds used here. For a given cloud top height, the cloud top temperature does generally slightly increase with  $N_a$  due to warming of the upper troposphere (Fig. 10 in the main text). However, here again the change is non-monotonic and non SST- and threshold-consistent (Fig R1a, c and e). Thus, we conclude that changes in the cloud top temperature and height with aerosols do not significantly affect the radiation budget.

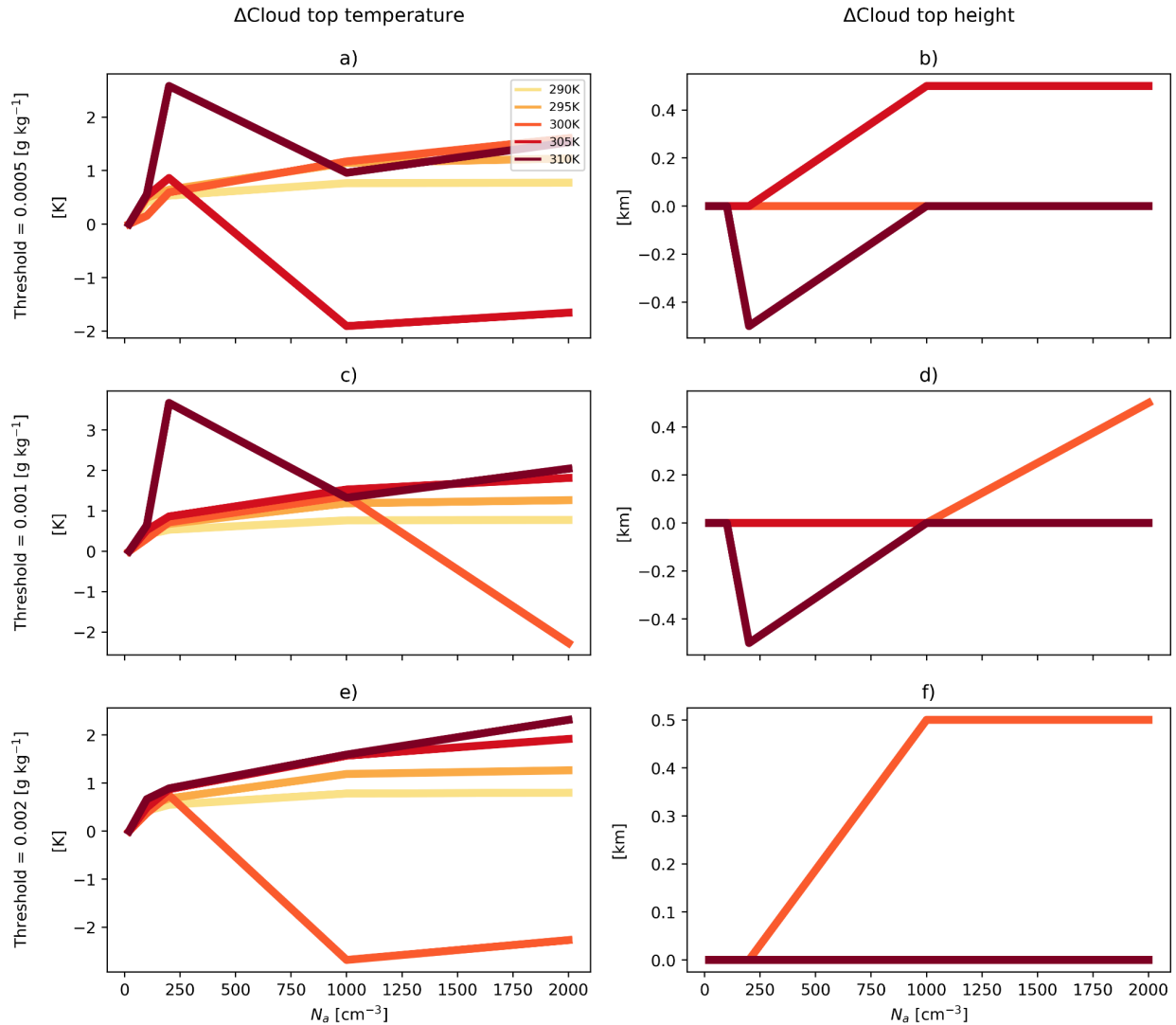


**Figure R1.** The response of domain and time mean cloud top temperature (left column) and cloud top height (right column) to an increase in  $N_a$ , both for three threshold choices:  $0.5 \cdot 10^{-3} \text{ [g kg}^{-1}\text{]}$  (first row),  $1 \cdot 10^{-3} \text{ [g kg}^{-1}\text{]}$  (second row) and  $2 \cdot 10^{-3} \text{ [g kg}^{-1}\text{]}$  (third row). The values are presented relative to the cleanest run ( $N_a = 20 \text{ cm}^{-3}$ ) for each SST, as indicated by the  $\Delta$  sign.

2. While this is clearly an idealized study, I am not convinced that using the  $N_a$  of 20/cc is the best choice. To my knowledge, the  $N_a$  should be higher even under very clean conditions.

**Reply:** Thank you. Indeed, this is an idealized study and the use of a wide range of  $N_a$  conditions serves to better understand the physics. However, according to a recent observational based data set of CCN

(Choudhury and Tesche, 2023), in the boundary layer (height of 500 m above the surface) the 5th to 95th percentile range of  $N_a$  (evaluated in this case at 0.2% supersaturation) is 19.9 to 1943.7  $\text{cm}^{-3}$  based on the global coverage and all the times available, i.e., almost exactly the range that is simulated here.

Following this comment we have added the following to the revised methods : “ $N_a$  ranges from 20 to 2000  $\text{cm}^{-3}$  ..., following a recent observational data set (Choudhury and Tesche, 2023), which showed the feasibility of this  $N_a$  range.”

In addition, we note that other references reported such low  $N_a$  conditions ( $<20 \text{ cm}^{-3}$ ) in remote locations (Flores et al., 2021).

3. Could lower aerosol radiative sensitivities at warmer temperatures be explained simply by an overall reduction in clouds (both anvil and low cloud fractions decrease at warmer temperatures), and thus a reduction in the domain-averaged effects of aerosol-cloud interactions?

**Reply:** We thank the reviewer for this comment. Indeed, SST-driven change in the baseline cloud fraction plays a significant role in the SST-sensitivity of the response to an increase in  $N_a$ . This is now demonstrated and explained in the revised manuscript. Please see our answer to comment 1 above.

4. Intuitively, I would expect more smaller ice crystals in polluted deep convective clouds. These would, at least holding everything else constant, lead to an increase in the anvil cloud fraction. Do anvil microphysical properties change under high aerosol conditions?

If the above is true, these changes seem to play only a second order role compared to the stability iris mechanism.

Does this mean that the aerosol-cloud interaction community shouldn't overemphasize the direct effects of aerosols on cloud properties, but rather think about cloud adaptations?

Moreover, the thermodynamic changes that drive these adjustments may be easier to understand (or at least more accessible to a broader community). Another implication may be that we shouldn't worry too much about getting all the microphysical details right.

**Reply:** Thank you. Indeed, increasing aerosol concentration could increase the lifetime of anvils, as was previously shown, for example by Grabowski and Morrison, 2016. In our simulations, under high aerosol conditions there are smaller ice crystals, which sediment slower from the cloud (ice sedimentation flux becoming more positive, see Fig. S11, SI below), thus acting to increase the anvil’s life time. However, in this paper we show that ice cloud fraction decreases with aerosols, i.e., the opposite effect. Thus, we can conclude that in our simulations the smaller sedimentation flux plays a secondary role in ice cloud fraction changes with aerosols.

The figure below was added to the SI and a clarification was added to the manuscript: “*In addition to modifying  $D_r$ , an increase in  $N_a$  also affects the lifetime of anvil clouds by perturbing the sedimentation rate (Grabowski and Morrison, 2016). Specifically, high aerosol conditions lead to smaller ice crystals, which sediment slower from the cloud (i.e. the sedimentation flux becomes less negative; Fig. S11, SI), thus acting to increase  $CF_{ice}$ . However, Fig. 5a shows a decrease in  $CF_{ice}$  with  $N_a$  in our simulations, thus making this to be only a secondary effect compared with the effect of  $D_r$  (agreeing with previous results regarding the effect of warming on anvil clouds (Beydoun et al., 2021))*”

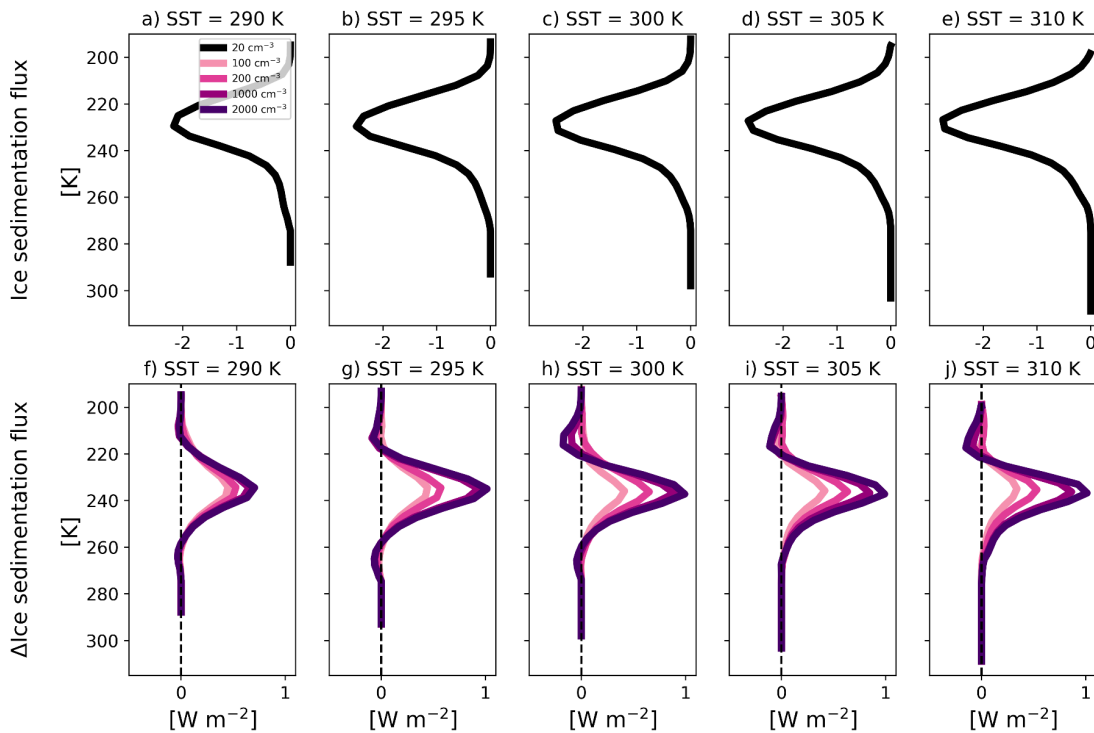


**Figure S11.** Domain and time mean vertical profiles of ice sedimentation flux for the cleanest run for each SST ( $N_a = 20 \text{ cm}^{-3}$ ; **a-e**), and its response to an increase in  $N_a$  relative to the cleanest run for each SST (**f-j**).

Regarding the reviewer's comment about the fact that these results suggest that the aerosol-cloud interaction community shouldn't overemphasize the direct effects of aerosols on cloud properties, but rather think about cloud adaptations, we very much liked this idea and found it intriguing. However, we have decided to wait for the RCEMIP-ACI results to see if this is a robust feature of all models in order to make this claim in a paper.

5. Several plots should be improved:

-Fig. 1 and 4: I suggest adding markers for better line visibility (or thicker lines, or both)

-Fig. 2,3,5,8,9: add zero line where appropriate (where anomalies cross it)

-Fig. 3,5: please use same x-axis limits if possible.

**Reply:** Thank you. Following your suggestions, we thickened the line in Fig. 1 and 4 (now Figs. 1 and 2, respectively), added zero dashed lines in Figs. 3, 5, 8, 9 (now Figs. 3, 7, 10, 11 respectively) where appropriate, and used the same x-axis in Fig. 3. We didn't use the same x-axis in Fig. 5 (now Fig. 7) since the axes have different orders of magnitude between each other. Fig. 2 was removed due to revisions in the manuscript.

**Specific comments:**

1. Page 1, line 5:

“decline in TOA energy gain”

I think this can be written in simpler words

**Reply:** The sentence was rewritten for clarity: “*Notably, changes in cloud radiative effects for both the longwave and shortwave parts of the spectrum lead to a decrease in top-of-atmosphere (TOA) energy gain with increasing  $N_a$ .*”

2. Page 2, line 57:

I suggest to remove “general”

**Reply:** The word "general" has been removed.

3. Page 3, line 80:

Something is odd/missing there.

**Reply:** Thank you, the sentence was rewritten for clarity: “*While observations, global climate models and high-resolution, convective-permitting models predict an increase in altitude of anvil clouds while maintaining nearly fixed temperatures, they also anticipate a decrease in anvil cloud coverage with rising surface temperatures.*”

4. Page 4, line 89-90:

Changes in ozone heating could also influence anvils (e.g. Harrop and Hartmann, 2012; Seidel and Yang, 2022)

**Reply:** Thank you. We agree with the reviewer. Following this comment a caveat was added to the methods section: “*A fixed ozone profile, representing a typical tropical atmosphere, is used here. We note that using a fixed ozone profile under different SST is not entirely realistic and may have some effect on the clouds’ development (Harrop and Hartmann, 2012; Seidel and Yang, 2022).*”

5. General comment on the introduction: are there similar studies that looked at aerosol impacts in RCE? If yes, please mention them, if not, please state that this is the first one looking at it.

**Reply:** Several other studies looked at aerosol impacts in RCE, and following your comment are mentioned in the introduction: “*This is done following previous studies that uses RCE to examine different aspects of ACI (van den Heever et al., 2011; Storer and van den Heever, 2013; Beydoun and Hoose, 2019; Dagan, 2022).*”

6. Page 4, Model description:

Anvils are ice phase clouds that strongly depend also on how freezing is parameterized in the model. Please add information also about the ice phase microphysics!

**Reply:** Thank you. Following this comment we added information about the ice phase microphysics: “Here, ice nucleation is not directly coupled to  $N_a$  (i.e., changes in  $N_a$  do not change the concentration of ice nucleating particles- INP), but rather depends on the temperature and the supersaturation with respect to ice (Rasmussen et al., 2002). We note that, in realistic conditions, changes in  $N_a$  might cause changes in INP, an effect that should be addressed in future research. In our simulations, heterogeneous nucleation dominates for temperatures higher than approximately 238 K, while ice formation is dominated by homogeneous freezing for temperatures lower than approximately 233 K (Rasmussen et al., 2002). Ice nucleation directly from vapor is not considered here.”

7. Page 4, Experimental design:

Is the ozone heating profile fixed? If so, I suspect anvils may already be influenced by it in the warmest experiment.

**Reply:** Thank you. Please refer to our answer to comment 4.

8. Page 6, line 141:

“clouds become thicker” Do the authors mean thicker in optical sense, or simply that their vertical extent is larger?

**Reply:** We meant that the clouds' vertical extent is larger, but due to the revisions made in the paper it's no longer relevant.

9. Page 7 & 8, Fig. 2 & 3:

With the upward shift in clouds a kg of air covers a larger volume. The increase of cloud ice/upper tropospheric cloud water may therefore not be consistent with the changes in integrated amount of ice. Does ice water path change across the investigated range of SSTs?

**Reply:** Thank you for this important question. As can be seen in the figure below,  $\mathcal{I}$  changes with SST in a non-monotonic manner. Understanding this interesting trend requires further investigation



that's out of the scope of this article, which examines the effect of  $N_a$  on cloud development under different SSTs rather than the effect of SST. Thus, this interesting question should be looked at in future research.

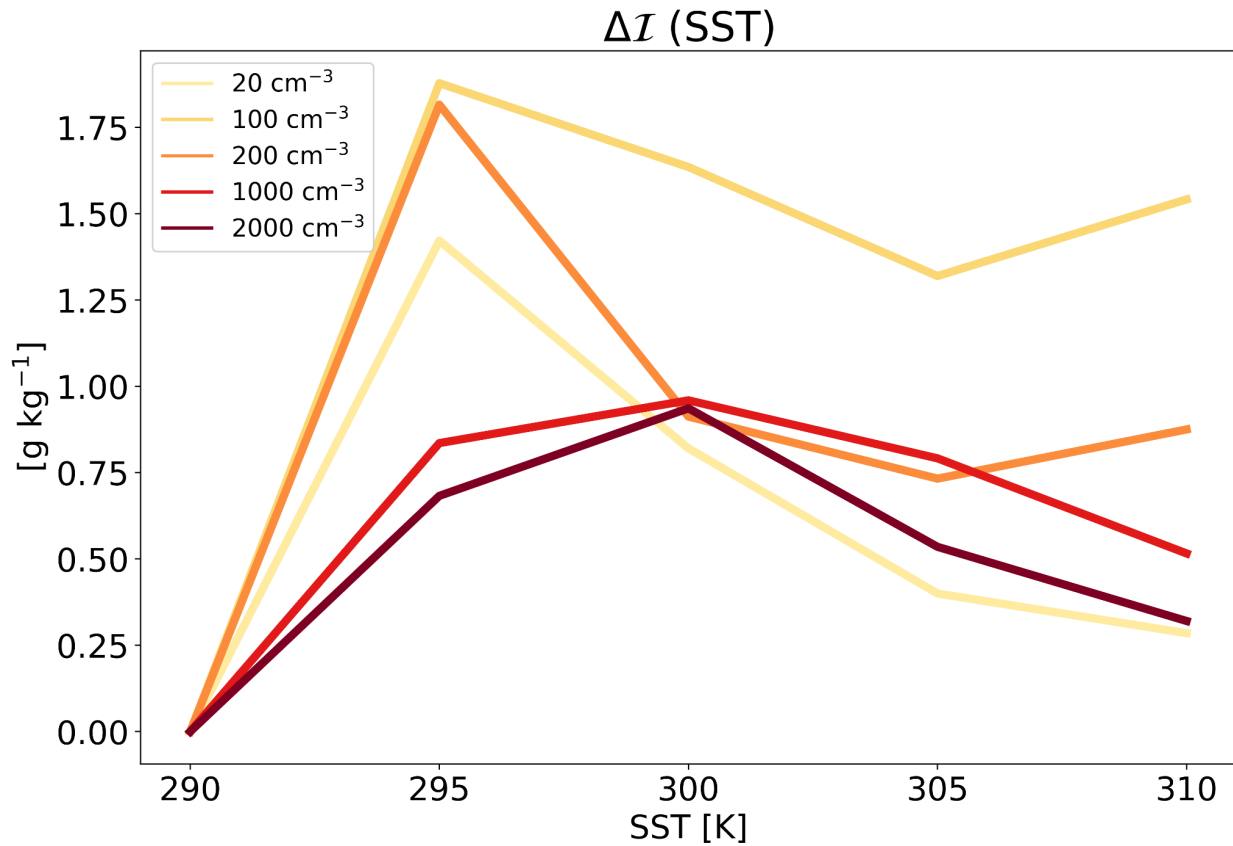


**Figure R2.** The response of domain and time mean ice water path ( $\mathcal{I}$ ) to an increase in SST. The values are presented relative to the coldest run (SST = 290 K) for each  $N_a$ , as indicated by the  $\Delta$  sign.

10. Page 9, lines 193-194:

Do changes in graupel production really explain the warming in the upper troposphere? Peak warming seems to be at higher altitudes.

**Reply:** At 240-220K level, graupel and snow increase with  $N_a$ . At these temperature levels we also see an increase in latent heating (Fig. S8, S1). In higher altitudes, the air density drops. Thus, a given amount of latent heating will cause a bigger temperature change at higher altitudes than low altitudes (Gasparini et al., 2023), which can explain why peak warming seems to happen at higher altitudes than peak latent heating release. Following this comment a clarification was added: “*In addition, in higher*

altitudes, the air density drops. Thus, a given amount of latent heating will cause a larger temperature change at higher altitudes than low altitudes (Gasparini et al., 2023).”

11. Page 10, lines 205-208:

It may be useful to decompose the within atmospheric heating to the cloudy and clear-sky parts. Or just clearly state that the total heating and the anomalies described here are driven by clear-sky radiative cooling.

**Reply:** Thank you. As was shown above,  $CF_{ice}$  reduces with  $N_a$ , driving an increase of the amount of clear-sky grid points. Thus, LWC is indeed driven by clear-sky radiative cooling, which is in turn driven by changes in the cloud fraction. The additions to the manuscript following this comment: “*The enhanced  $\Delta LWC$  with  $N_a$  is driven by clear-sky radiative cooling, which is in turn driven by the decreased  $CF_{ice}$  with  $N_a$  across SSTs, as illustrated in Fig. 5a. The enhanced  $\Delta LWC$  is also consistent with the reduction in  $\Delta R^{LW}$  presented in Fig. 1b.*”

12. Page 11, Fig. 9:

How should we interpret the increase in advective tendency of the liquid/ice water static energy?

**Reply:** Thank you for this question. The increase in advective tendency of the liquid/ice water static energy is a response to an increase in latent heating. For a certain height, an increase in latent heating drives an increase in the amount of heat that will be advected from this height.

13. Page 16:

The authors could mention two more caveats:

- a. The assumed sensitivities do not include sensitivities related to changes in ice nucleation and freezing. A polluted environment would most likely lead not only to large numbers of CCN, but also to large numbers of ice nucleating particles and/or ice nucleating particles that freeze at warmer temperatures. This could lead to significant climate impacts that could easily match those described in this paper.

**Reply:** Thank you. Please refer to our answer to comment 6.

- b. Although tropical oceanic convection doesn't have as strong a diurnal cycle as land convection, its effects cannot be neglected. If the main aerosol-mediated changes in SW radiation are indeed those in deep convective cores, they may be muted in simulations with a diurnal cycle due to the early morning peak in deep convective activity (e.g. Nesbitt and Zipser, 2003; Gasparini et al. 2022).

**Reply:** Thank you, a caveat was added to the methods section: “*A diurnal cycle is not considered here, and we note that it might affect the convective development to some extent even over the ocean (Nesbitt and Zipser, 2003; Gasparini et al., 2022).*”

## References

- Beydoun, H., and C. Hoose. “Aerosol-Cloud-Precipitation Interactions in the Context of Convective Self-Aggregation.” *Journal of Advances in Modeling Earth Systems*, vol. 11, 2019, pp. 1066-1087, <https://agupubs.onlinelibrary.wiley.com/doi/abs/10.1029/2018MS001523>.
- Beydoun, Hassan, et al. “Dissecting anvil cloud response to sea surface warming.” *Geophysical Research Letters*, vol. 48, 2021.
- Bony, S., et al. “On dynamic and thermodynamic components of cloud changes.” *Climate Dynamics*, 2004, <https://doi.org/10.1007/s00382-003-0369-6>.
- Choudhury, G., and M. Tesche. “A first global height-resolved cloud condensation nuclei data set derived from spaceborne lidar measurements.” *Earth System Science Data*, vol. 15, 2023, 3747--3760, <https://essd.copernicus.org/articles/15/3747/2023/>.
- Dagan, Guy. “Equilibrium climate sensitivity increases with aerosol concentration due to changes in precipitation efficiency.” *Atmospheric Chemistry and Physics*, vol. 22, 2022, 15767--15775.
- Flores, J.M., et al. “Diel cycle of sea spray aerosol concentration.” *Nature Communications*, 2021, <https://doi.org/10.1038/s41467-021-25579-3>.

- Gasparini, Blaž, et al. “Basic physics predicts stronger high cloud radiative heating with warming.” 2023, <https://doi.org/10.21203/rs.3.rs-2772229/v1>.
- Gasparini, Blaž, et al. “Diurnal Differences in Tropical Maritime Anvil Cloud Evolution.” *Journal of Climate*, vol. 35, 2022, pp. 1655 - 1677, <https://journals.ametsoc.org/view/journals/clim/35/5/JCLI-D-21-0211.1.xml>.
- Grabowski, Wojciech W., and Hugh Morrison. “Untangling microphysical impacts on deep convection applying a novel modeling methodology. Part II: Double-moment microphysics.” *Journal of the Atmospheric Sciences*, vol. 73, 2016, 3749--3770.
- Harrop, Bryce E., and Dennis L. Hartmann. “Testing the Role of Radiation in Determining Tropical Cloud-Top Temperature.” *Journal of Climate*, vol. 25, 2012, pp. 5731 - 5747, <https://journals.ametsoc.org/view/journals/clim/25/17/jcli-d-11-00445.1.xml>.
- Nesbitt, Stephen W., and Edward J. Zipser. “The Diurnal Cycle of Rainfall and Convective Intensity according to Three Years of TRMM Measurements.” *Journal of Climate*, vol. 16, 2003, pp. 1456 - 1475, [https://journals.ametsoc.org/view/journals/clim/16/10/1520-0442\\_2003\\_016\\_1456\\_tdcora\\_2.0.co\\_2.xml](https://journals.ametsoc.org/view/journals/clim/16/10/1520-0442_2003_016_1456_tdcora_2.0.co_2.xml).
- Rasmussen, Roy M., et al. “Freezing Drizzle Formation in Stably Stratified Layer Clouds: The Role of Radiative Cooling of Cloud Droplets, Cloud Condensation Nuclei, and Ice Initiation.” *Journal of the Atmospheric Sciences*, vol. 59, 2002, pp. 837 - 860, [https://journals.ametsoc.org/view/journals/atsc/59/4/1520-0469\\_2002\\_059\\_0837\\_fdfiss\\_2.0.co\\_2.xml](https://journals.ametsoc.org/view/journals/atsc/59/4/1520-0469_2002_059_0837_fdfiss_2.0.co_2.xml).
- Seidel, Seth D., and Da Yang. “Temperatures of Anvil Clouds and Radiative Tropopause in a Wide Array of Cloud-Resolving Simulations.” *Journal of Climate*, vol. 35, 2022, pp. 8065 - 8078, <https://journals.ametsoc.org/view/journals/clim/35/24/JCLI-D-21-0962.1.xml>.
- Sokol, Adam B., et al. “Anvil cloud thinning implies greater climate sensitivity.” 2024, [https://atmos.uw.edu/~abs66/docs/Sokol\\_et\\_al\\_2024\\_preprint.pdf](https://atmos.uw.edu/~abs66/docs/Sokol_et_al_2024_preprint.pdf).

Storer, Rachel L., and Susan C. Van den Heever. "Microphysical Processes Evident in Aerosol Forcing of Tropical Deep Convective Clouds." *Journal of the Atmospheric Sciences*, vol. 70, 2013, pp. 430 - 446, <https://journals.ametsoc.org/view/journals/atsc/70/2/jas-d-12-076.1.xml>.

Twomey, Sean. "The influence of pollution on the shortwave albedo of clouds." *Journal of the atmospheric sciences*, vol. 34, 1977, 1149--1152.

van den Heever, Susan C., et al. "Aerosol Indirect Effects on Tropical Convection Characteristics under Conditions of Radiative–Convective Equilibrium." *Journal of the Atmospheric Sciences*, vol. 68, 2011, pp. 699 - 718, <https://journals.ametsoc.org/view/journals/atsc/68/4/2010jas3603.1.xml>.

Wing, Allison A., et al. "Clouds and convective self-aggregation in a multimodel ensemble of radiative-convective equilibrium simulations." *Journal of advances in modeling earth systems*, vol. 12, 2020.

## Reviewer #2

We would like to thank Reviewer #2 for their constructive suggestions. Please find below a point-by-point reply to all the referee's comments (in blue).

This is an interesting and useful study that examines how the assumed aerosol concentration  $N_a$  impacts cloud characteristics for a variety of sea surface temperatures (SST's) in idealized radiative-convective equilibrium simulations. This study builds on previous studies that focused on either the SST effect on clouds or the aerosol effect on clouds, but not the combination of both effects. It is shown that increased aerosol concentrations enable liquid cloud droplets to loft higher in the atmosphere as they do not grow and rain out as quickly. For the cooler simulations, which have shallower warm layers, droplets are lifted above the freezing level before the droplets are large enough to form rain. This decreases rain rates but increases ice crystal growth and therefore frozen precipitation production. For the warmer simulations, thicker warm layers allow rain to still form, although at higher elevations, and so the precipitation phase is not as sensitive to  $N_a$ . This finding was made possible because the study considered both a range of both SST's and values of  $N_a$ , rather than one or the other, which illustrates the novelty of the study. Interpretation of some of the results is problematic, which I have outlined further below. In particular, a central result of the study was that anvil cloud fraction is reduced with increasing  $N_a$ , but the authors do not clearly state how anvil cloud fraction is calculated and two plots showing anvil cloud fraction are inconsistent with each other. Furthermore, one plot appears to show anvil height changes with increasing  $N_a$ , but anvil coverage does not. Both observations call the anvil result into question. The authors may need to revisit their analysis of simulation output in order to correct the inconsistency in the anvil cloud fraction. If the results change, the discussion and conclusions may need to be significantly revised. There are also some smaller claims that appear to be unsupported in plots, outlined below, which also necessitate a revision of some of the results/discussion and conclusion sections. Once the issues with anvil cloud fraction are addressed, I believe there is significant potential for novel results about anvils that would attract a wide audience. In particular, it is possible that both FAT and the stability iris hypothesis are supported for a given  $N_a$ , but FAT does not apply across different  $N_a$ . Rather, increased  $N_a$  raises and thins anvils. These guesses are based off a tenuous reading of the plots and would need to be examined further.

## General comments

1. The claim that increasing  $N_a$  decreases anvil cloud fraction (CF) is first made a line 157, in reference to Fig. 2c. Fig. 2a shows a maximum in CF at about 220K, and Fig. 2c shows increases in CF above this level and decreases below with increasing  $N_a$ . This indicates a rising of the level of maximum CF. The increase in CF above 220K is smaller in magnitude than the decrease in CF between 250K and 220K, which indicates the anvil depth decreases with an increase in  $N_a$ . Furthermore, if the zero-crossing in plot 2c is precisely at or below the maximum in plot 2a, as it appears, the value of the maximum CF could not be decreasing. However, it is difficult to tell in the plots. Anvil CF is further investigated at line 161 and Fig. 6a, which shows a relationship between anvil CF and maximum mass divergence. The plots are inconsistent given that all points in Fig. 6 have anvil CF < 0.24 but that all profiles in Fig. 2a have a maximum CF > 0.35 at about 220K. The authors need to describe carefully how anvil CF is calculated. My guess is that, for Fig. 6, anvil cloud fraction is calculated as the time mean of (number of cloudy grid points above 245K) / (total number of grid points above 245K). This is not the anvil cloud fraction, but rather the anvil cloud volume. If true, this would explain why Fig. 6a shows a decrease in anvil CF, but Fig 2 does not: anvil depth decreases, decreasing their volume, but not necessarily their horizontal extent. The authors should calculate anvil cloud fraction as the maximum in the vertical profile of cloud fraction above 245K, which would be the same definition as Beydoun et al., 2021 and similar to the definition in Saint-Lu et al., 2020.

**Reply:** Thank you very much for raising this important point that made us look deeper into the changes in anvil cloud fraction and its distribution. Following this comment significant modifications were implemented into the revised manuscript as elaborated below. Specifically, following this comment, and a comment from reviewer #1, we have adopted the perspective presented in Sokol et al., 2024, which examines the ice cloud fraction ( $CF_{ice}$ ) as a continuum of clouds with different ice depth rather than as entities with fixed depth. However, unlike Sokol et al., 2024, which looks only at ice clouds, here we are interested in both liquid and ice clouds. Thus, instead of looking only at the ice distribution, we are examining 2D histograms of liquid water path ( $\mathcal{L}$ ) and ice water path ( $\mathcal{I}$ ), and the response of these histograms to changes in  $N_a$ . The figure below, which was added to the revised manuscript as Fig. 4, presents the 2D histograms of the occurrence of cloud fraction (CF) at the different bins of  $\mathcal{L}$  and  $\mathcal{I}$  and the average total, shortwave and longwave cloud radiative effect (CRE) at these different bins. These quantities are presented for two simulations using the lowest ( $20 \text{ cm}^{-3}$ ; panels a-d) and the highest ( $2000 \text{ cm}^{-3}$ ; panels e-h)

$N_a$  under SST = 290 K. In addition, the difference between the high and low  $N_a$  conditions is presented in panels i-l. This figure demonstrates that the CF in these RCE simulations is dominated by anvil clouds (e.g. Wing et al., 2020), i.e., clouds with negligible  $\mathcal{L}$  and high (thick anvil clouds; denoted by marker 1 in Fig. 4a) or low (thin anvil clouds; denoted by marker 1 in Fig. 4a)  $\mathcal{I}$ . However, Fig. 4 also demonstrates the existence of 2 other types of clouds in these RCE simulations - shallow clouds (high  $\mathcal{L}$  and low  $\mathcal{I}$ ; denoted by marker 3 in Fig. 4a) and deep convective cores (high  $\mathcal{L}$  and high  $\mathcal{I}$ ; denoted by marker 4 in Fig. 4a). Examining the difference between the high and low  $N_a$  simulations demonstrates that the reviewer was right and that an increase in  $N_a$  derives a thinning of the anvil clouds, i.e., an increase in the frequency of thin anvil clouds and a decrease in the frequency of thick anvil clouds (Fig. 4i). It also demonstrates that with the increase in  $N_a$  the CRE becomes more negative for all  $\mathcal{L}$  and  $\mathcal{I}$  (and especially for low  $\mathcal{I}$  and medium-high  $\mathcal{L}$ ; Fig. 4j) bins, driven mostly by changes in the SW (Fig. 4k), with only a minor change in the LW (Fig. 4l). This trend is driven by the Twomey effect (Twomey, 1977). This interesting trend is now presented and discussed in the revised manuscript, which we believe improved the contribution of our paper. Thus, we are grateful that the reviewer brought this point up.

In addition to the continuum perspective presented in Fig. 4, we examine the trend in the total  $CF_{ice}$  with  $N_a$ , which is calculated by integrating over thick ice plus thin ice regimes as defined in Table S1, SI (see below; see also Sokol et al., 2024). This calculation demonstrates that, as was reported in the original manuscript, the  $CF_{ice}$  is reduced with an increase in  $N_a$  for all the SST examined here (Fig. 5a). This new and well described definition of  $CF_{ice}$ , supports our original findings. In the revised manuscript we use this definition for  $CF_{ice}$ .

The additions to the revised manuscript:

*“Figs. 1, 2, 3 examine the bulk cloud and radiative properties in the domain. However, as previously demonstrated, the impact of aerosols on clouds is cloud regime dependent (Gryspeerd and Stier, 2012; Christensen et al., 2016; Dagan and Stier, 2020b). Therefore, it is crucial to analyze the distribution of cloud regimes in our simulations and discern how each specific cloud regime responds to the increase in  $N_a$ . In this paper we define the cloud regimes based on different bins of  $\mathcal{L}$  and  $\mathcal{I}$ . For that purpose, Fig. 4 presents 2D histograms of the cloud fraction (CF), or cloud occurrence, at the different bins of  $\mathcal{L}$  and  $\mathcal{I}$  and the average total, shortwave and longwave CRE at these different bins, all for the coldest case considered here (SST = 290 K) as an example. This figure illustrates that the CF in these RCE simulations is mostly dominated by anvil clouds (e.g. Wing et al., 2020), i.e., clouds with negligible  $\mathcal{L}$  and high (thick anvil clouds; denoted by marker 1 in Fig. 4a) or low (thin anvil clouds; denoted by marker 2 in Fig. 4a)  $\mathcal{I}$ . We note that the average*



CRE of thin anvil cloud is small but not positive as in previous assessments (Sokol, 2024), probably due to the use of a relatively coarse resolution of  $\mathcal{L}$  and  $\mathcal{I}$  bins. However, Fig. 4a also illustrates the existence of two other types of clouds in these RCE simulations - shallow clouds (high  $\mathcal{L}$  and low  $\mathcal{I}$ ; denoted by marker 3 in Fig. 4a) and deep convective cores (high  $\mathcal{L}$  and high  $\mathcal{I}$ ; denoted by marker 4 in Fig. 4a). In addition, Fig. 4 i-l illustrates the difference between simulations with the highest ( $2000 \text{ cm}^{-3}$ ) and the lowest ( $20 \text{ cm}^{-3}$ )  $N_a$  conditions. Specifically, Fig. 4i illustrates that an increase in  $N_a$  drives thinning of the anvil clouds, i.e., an increase in the frequency of thin anvil clouds and a decrease in the frequency of thick anvil clouds. Furthermore, Fig. 4 j-l illustrate that with an increase in  $N_a$  the CRE decreases for all  $\mathcal{L}$  and  $\mathcal{I}$  bins (and especially for medium-high  $\mathcal{L}$  and low  $\mathcal{I}$ ; Fig. 4j), driven mostly by changes in the SW (Fig. 4k), with only minor changes in the LW (Fig. 4l). This SW difference with  $N_a$  can be explained by the Twomey effect (Twomey, 1974). Following the method outlined in (Sokol, 2024), we calculate the total ice cloud fraction ( $CF_{ice}$ ) as the integral over thick ice plus thin ice regimes as defined in Table S1, SI. Fig. 5a illustrates a (mostly) monotonic decrease across SSTs in  $CF_{ice}$  with increasing  $N_a$ , consistent with the domain mean CF reduction (Fig. 2c). We note that not just the integrated  $CF_{ice}$  decreases with  $N_a$ , but the entire distribution of  $\mathcal{I}$  is shifted to lower values (i.e., thinning of the anvil clouds; Figs. 4i, 2b and 3h). A decrease in  $CF_{ice}$  leads to more outgoing LW radiation out of the atmosphere and reduces  $\Delta R^{LW}$ , as can be seen in Fig. 1b. In addition, Fig. 5b presents the relative change in the shallow cloud fraction ( $CF_{shallow}$ ; calculated as the integral over the shallow regime as defined in Table S1, SI). We note that this definition of shallow clouds might also include two-layer cloud conditions with cirrus clouds with relatively low  $\mathcal{I}$  above shallow clouds. Figure 5b illustrates a rise in  $CF_{shallow}$  with  $N_a$  for low SST, while for high SST it illustrates a decrease in  $CF_{shallow}$  with  $N_a$  (the change in the shallow cloud fraction is not observed in Fig. 4i due to the dominance of ice clouds, which inflates the color-bar range). We note that although the relative changes in  $CF_{ice}$  and  $CF_{shallow}$  has similar magnitudes, the baseline (i.e., referring to the simulated value, and not the difference between the most polluted and cleanest runs)  $CF_{ice}$  is two orders of magnitude larger than  $CF_{shallow}$  (Fig. S6, SI).”

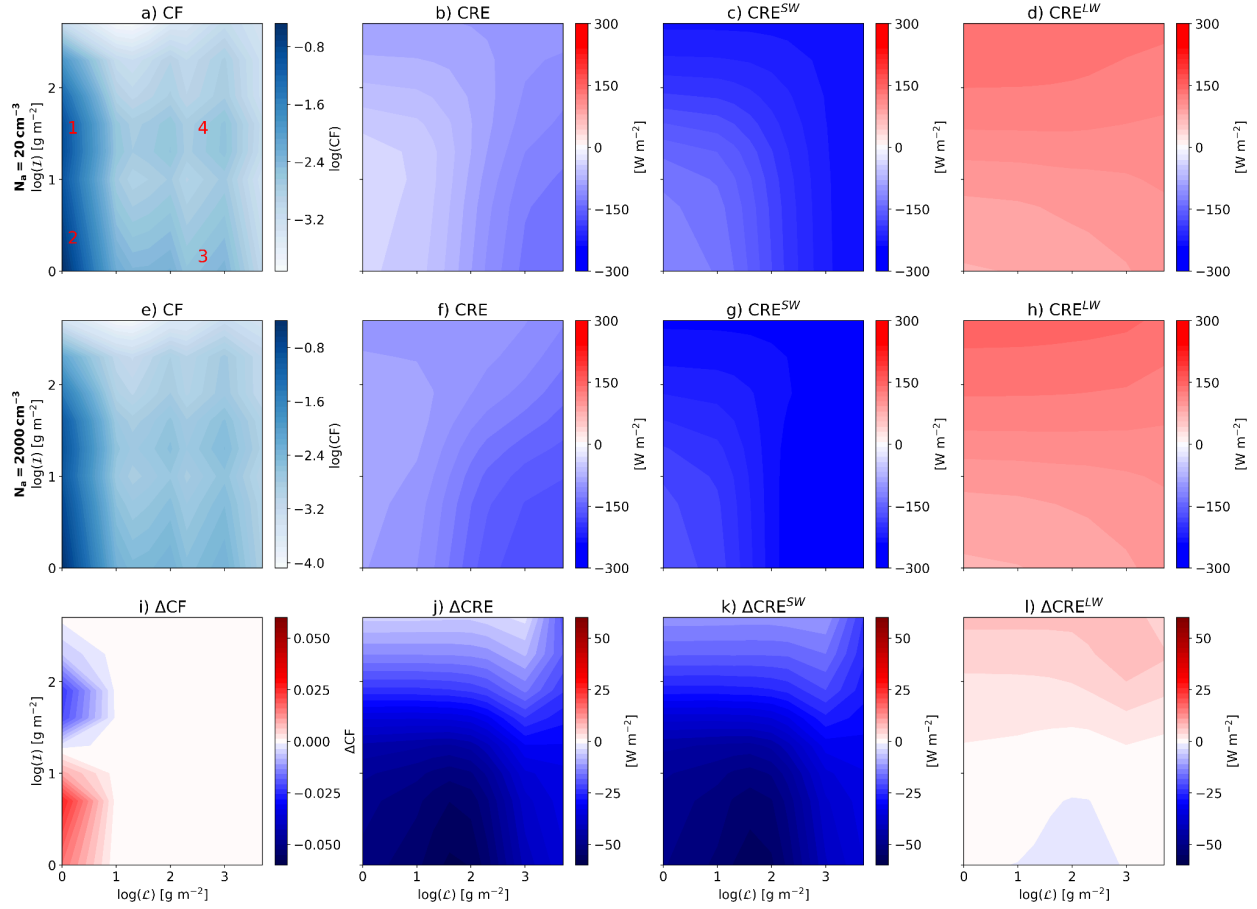


**Figure 4.** Domain and time mean two-dimensional histograms of cloud fraction (CF; **a** and **e**), at different bins of liquid water path ( $\mathcal{L}$ ) and ice water path ( $\mathcal{I}$ ) and the average total (**b** and **f**), shortwave (**c** and **g**) and longwave (**d** and **h**) cloud radiative effect (CRE) at these different bins. These quantities are presented for two simulations using the lowest ( $N_a = 20 \text{ cm}^{-3}$ ; **a-d**), and the highest ( $N_a = 2000 \text{ cm}^{-3}$ ; **e-h**)  $N_a$ , under SST = 290 K. In addition, the difference between the highest and lowest  $N_a$  conditions is presented in panels **i-l**.

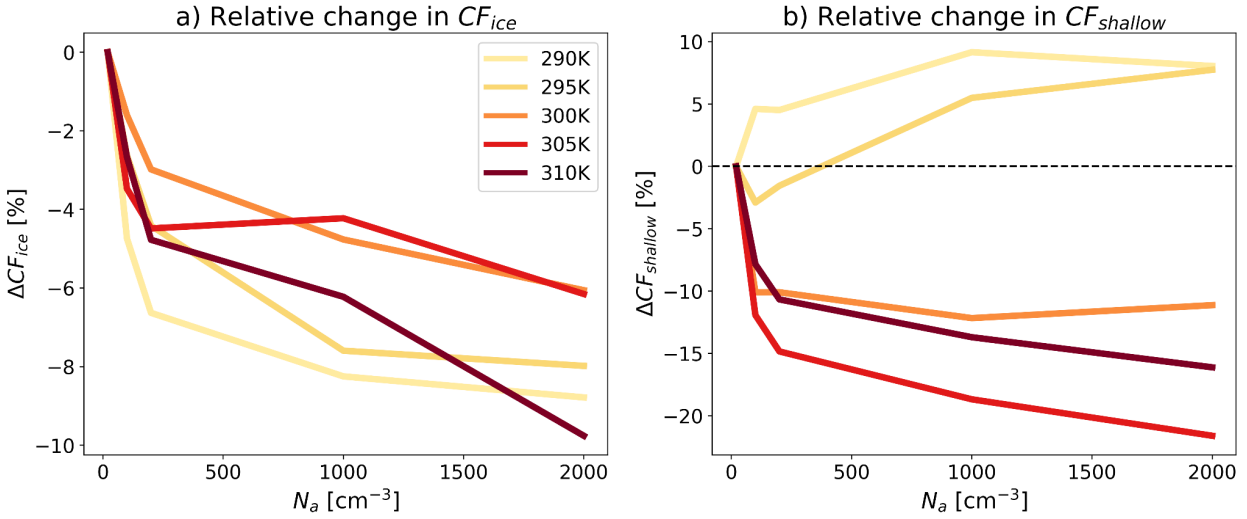


**Figure 5.** The relative response of domain and time mean ice cloud fraction ( $CF_{ice}$ ; **a**) and shallow cloud fraction ( $CF_{shallow}$ ; **b**) to an increase in  $N_a$ . The values are shown as a difference, relative to the cleanest run (as denoted by the  $\Delta$  sign), for each SST. The baseline  $CF_{ice}$  and  $CF_{shallow}$  are presented in Fig. S6, SI.

2. In multiple locations, a distinction is made between the cloud radiative effect specifically and the overall changes to radiative effects generally. But aerosols were only allowed to change cloud microphysics and not interact with radiation directly, and thus the CRE was effectively the only thing that was allowed to change in the simulations. Indeed, the top and bottom rows in Fig. 1 appear nearly identical. Specifically, the following statements are misleading and should be reworded:

- L5: “we show that increasing  $N_a$  leads to a decline in top-of-atmosphere (TOA) energy gain across SSTs due to changes in the cloud radiative effect”
- L130: “the CRE ... is identified as the main driver of  $\Delta R$  variations, while changes in clear sky radiation has a minimal impact”
- L218: “increasing  $N_a$  decreases top-of-atmosphere (TOA) energy gain ... as a result of changes in the cloud radiative effect.”

In all cases, I suggest it be made clear that the aerosol concentration affects the CRE, which is the only component of the overall aerosol radiative effect that is examined.

**Reply:** Thank you for this comment. Indeed, aerosols were allowed to affect clouds but not directly affect radiations (i.e., aerosol-radiation interactions are excluded). Following the reviewer comment, we made sure that this is clear through the manuscript.

- a. We understand the reviewer's point, but we think that mentioning that aerosol-radiation interactions are excluded doesn't belong in the abstract. We explicitly mentioned this important point in the next two instances.
- b. This sentence was changed to: *“Moreover, the CRE (calculated as all sky radiative flux minus clear sky radiative flux) is identified as the main driver of  $\Delta R$  variations, while changes in clear sky radiation has a minimal impact, as indicated by Fig. 1d-f. This is true in our simulations as changes in  $N_a$  do not directly affect radiation by aerosol-radiation interactions.”*
- c. This sentence was changed to: *“...we demonstrate that increasing  $N_a$ , which does not directly interact with radiation here, decreases top-of-atmosphere (TOA) energy gain”*

However, please note that as the thermodynamic conditions are changing with  $N_a$  (Fig. 10 in the main text), the clear-sky radiation is allowed to change, and in fact changes with  $N_a$  to some degree. The decomposition into cloudy and clear-sky serves to demonstrate that the clear-sky changes are minimal compared with the CRE changes.

3. The introduction presents a nice overview of research on how clouds respond to changes in SST, including the FAT hypothesis and the stability iris effect. There is also a nice overview of existing work on how aerosols affect cloud properties. However, while there is a clear motivation for investigating higher SST's, the reader may be left wondering how realistic the aerosol concentration scenarios used are, if and how global aerosol concentrations are expected to change under warming, and how the results of the study would modify the aerosol concentrations further. For example, the study finds increased aerosol concentrations may increase precipitation rates. One may hypothesize that such increased precipitation would feed back into the aerosol concentration as the aerosols get rained out faster, and thus moderate the concentration. Even if these effects are highly uncertain, they could be discussed.

**Reply:** The reviewer is correct that an increase in precipitation will feedback on the aerosol concentrations and that this feedback is not included in this study. Following this comment, a caveat was added to the revised conclusions section: *“We note that an increased surface precipitation could mean*

*that aerosols get rained out faster, thus moderating the aerosol concentration. In our simulations  $N_a$  is prescribed, thus this feedback is disabled. This feedback should be examined in future studies.”*

In addition, the use of a wide range of  $N_a$  conditions serves to better understand the physics. To demonstrate that the range of  $N_a$  conditions considered here is relevant to the real world, we use a new observational-based data set of CCN (Choudhury and Tesche, 2023), which states that in the boundary layer (at 500 m above the surface) the 5th to 95th percentile range of  $N_a$  (evaluated in this case at 0.2% supersaturation) is 19.9 to 1943.7  $\text{cm}^{-3}$  based on the global coverage and all the times available, i.e., almost exactly the range that is simulated here. Following this comment we have added the following to the revised methods section : “ $N_a$  ranges from 20 to 2000  $\text{cm}^{-3}$  (20, 100, 200, 1000, and 2000  $\text{cm}^{-3}$ ), following a recent observational data set (Choudhury and Tesche, 2023), which showed the feasibility of this  $N_a$  range.”

4. The supplement presents plots in the same format as the plots in the main text, but every plot has all combinations of SST and  $N_a$ . Including all 25 profiles on each plot makes them impossible to read. I would create a new plot for each value of  $N_a$  so that these plots can be read. The plots would be exactly as the top row (or only row) in Figs. 1,3,5,8,9, but for different  $N_a$ .

**Reply:** Thank you. Following this comment, the figures in the SI have been adjusted as suggested, but with a new plot for each SST instead for each  $N_a$ .

5. Most vertical profiles in the study are plotted with temperature as the vertical coordinate. I find this quite useful in some cases, e.g. fig 2a appears to support the FAT hypothesis. In other cases, it is slightly more confusing, e.g. in determining the altitude of rain production in figs. 3b and 3g. The only change I would request here is that there appears to be an artifact in most profiles that could be removed. For example, the cloud ice profile (Fig 3c) is bivalued between  $\sim 200\text{k}$  and  $\sim 230\text{K}$ . I assume one value is from the stratosphere while the other is from the troposphere. I suggest truncating the profiles where the temperature begins to increase, thus ensuring each T is uniquely associated with a single z.

**Reply:** Thank you. Following this comment we have updated all of the relevant figures in both the SI and the article, to ensure each T is uniquely associated with a single height. This was done by cutting the vertical profiles at the tropopause, defined as the level at which the temperature starts to rise with altitude.

### Specific comments

1. L5: “, even at equilibrium conditions.”: Things not at equilibrium include the SST with insolation and  $N_a$  with aerosol removal via deposition. I suggest explicitly stating the equilibrium is RCE.

**Reply:** Thanks. We have followed the reviewer's suggestion and updated this sentence as follows: “*Our results indicate that ACIs are SST-dependent even under RCE conditions.*”

2. L133: Please describe how grid points are defined as cloudy for the purpose of calculating cloud fraction

**Reply:** Please see our reply to general comment 1 and the new used definition for CF.

3. L135: Does “total water” refer only to total liquid and ice? If so, please clarify. “total water” to me reads as including water vapor.

**Reply:** Thank you. Indeed, “total water” refers to liquid and ice and not to vapor, i.e., total condensed water. Due to revisions made in the paper we no longer use total water, hence this is no longer relevant.

4. L146: “under lower SST ... an increase in  $N_a$  can completely suppress warm rain (see Fig. 3g).” This appears unsupported in the plot. The cleanest 290K run shows a maximum for rain of  $\sim 0.004\text{g kg}^{-1}$ , while the change in rain in the polluted scenario shows a maximum change of  $\sim -0.002\text{g kg}^{-1}$ . Please quantify this statement.

**Reply:** Thank you for raising this discrepancy. In the coldest simulations, a rise in  $N_a$  suppressed about 30% of the rain in the domain-mean vertical profile, while in the hotter simulations a rise in  $N_a$  suppressed about 10% of the rain in the entire domain. This calculation was done by integrating the rain vertical profiles of each simulation, followed by determining the difference between the most polluted ( $N_a = 2000\text{ cm}^{-3}$ ) and the cleanest ( $N_a = 20\text{ cm}^{-3}$ ) runs, relative to the cleanest run, for each SST. Following this comment we updated the sentence: “*under lower SSTs... an increase in  $N_a$  can inhibit warm rain (see Fig. 3g).*”

5. L151: “The stronger increase in total water with  $N_a$  under lower SSTs leads to the stronger SW reflectivity,”: I’m not sure that just the result of increased total water is enough to establish causality here, with the role of anvils and changes to cloud morphologies uncertain. Perhaps just “consistent with”.

**Reply:** Thank you. Due to revisions made in the paper this is no longer relevant.

6. L156: “higher  $N_a$  and lower SSTs ... thus producing more graupel (Fig. 3i)” In Fig. 3i, the coldest run shows the smallest increase in graupel production. The largest increase is from the middle 300K simulation, so there is not a clear trend.

**Reply:** Thank you for this comment. Following this comment, the sentence was rewritten to better describe the results presented in the figure: “Beside resulting in an increase in  $\mathcal{L}$ , the warm rain inhibition under higher  $N_a$  results in more super-cooled water (Carrió et al., 2011; Chen et al., 2017, Fig. 3f), leading to higher production of snow (Chen et al., 2017, Fig. 3j), and drives higher riming rates, thus producing more graupel (Chen et al., 2017, Fig. 3i).”

7. L169: “A reduction in  $D_r$  with  $N_a$  could be attributed to changes in  $Q_r$ ”: For me, it’s less intuitive that  $N_a$  would affect  $Q_r$  than  $D_r$ . Throughout this section, it is not clear to me that causality can be established, though I don’t understand the calculation. Please explain the calculation and consider whether it establishes causality.

**Reply:** Thank you. Throughout the section we explain that changes in  $D_r$  with  $N_a$  can be driven by changes in either  $Q_r$  or  $S$  with  $N_a$ , or both. To realize which ( $S$  or  $Q_r$ ) is responsible for the changes in  $D_r$  with  $N_a$  for the different SSTs, we calculate in Fig. 9 changes in  $D_r$  with  $N_a$ , assuming that either  $S$  or  $Q_r$  are fixed at a reference  $N_a$  of  $200 \text{ cm}^{-3}$ . That is to say that we took the vertical profile of  $S$  or  $Q_r$  from, for example, the simulations using  $\text{SST} = 300 \text{ K}$  and  $N_a = 200 \text{ cm}^{-3}$ , and used them to calculate the vertical profiles of  $D_r$  for all  $N_a$  conditions under SST of 300K. Then, we examined how  $D_r$  changes with  $N_a$ , assuming that  $S$  or  $Q_r$  are held fixed, for each SST. This calculation is similar to that in Bony et al., 2016, Fig. 4, but for changes in  $N_a$  instead of SST. Fig. 9 shows that  $D_r$  decreases monotonically with  $N_a$  when  $Q_r$  is held fixed, while  $D_r$  changes without a clear trend with  $N_a$  when  $S$  (or T) is held fixed. Since  $D_r$  decreases with  $N_a$  for a fixed  $Q_r$  but not when  $S$  is held fixed, a causality between the observed changes in  $S$  and the changes in  $D_r$  with  $N_a$  can be established.

8. L178: “for a given SST, an increase in  $N_a$  drives strong warming of the upper troposphere and a weak cooling of the lower troposphere.”: The two coldest simulations do not appear to cool in the lower troposphere. They warm in the upper troposphere, but both have small regions of cooling in the upper troposphere.

**Reply:** Thank you, the sentence was rewritten to better match the data presented: “*This figure illustrates that, for a given SST, an increase in  $N_a$  drives strong warming of the upper troposphere and in some cases a weak cooling of the lower troposphere.*”

9. L179: “the increase in  $S$  with  $N_a$  (Fig. 5a)”: Fig. 5a does not show the change with  $N_a$ , only the values for the cleanest simulation.

**Reply:** Thank you. The line was rewritten to better match the data presented: “*This trend demonstrates an increase in  $S$  with  $N_a$ , which in turn explains the reduction in the anvil cloud fraction.*”

10. L190: “driven by a stronger latent heat release,”: As well as weaker advection (since the advection term is negative), which appears to be a similar magnitude.

**Reply:** Thank you, the sentence was rewritten: “*...mostly driven by a stronger latent heat release...*”

11. L190: “is in turn driven by higher production rates of graupel and snow ”: I would say “consistent with”. The causality implied here is hard to see and may flow the other direction.

**Reply:** Thank you. We agree with the reviewer, and the sentence was rewritten as suggested: “*...which is consistent with the higher production rates of graupel and snow...*”

12. L199: Kirchoff’s Law implies  $\Delta LW C \approx -\Delta RLW$  because net surface LW radiation flux is zero if LW surface reflection is negligible. Is this true? The plots of  $\Delta LW C$  and  $-\Delta RLW$  appear almost identical.

**Reply:** This is indeed true, and is stated in the following paragraph: “*The enhanced  $\Delta LWC$  with  $N_a$  is driven by clear-sky radiative cooling, which is in turn driven by the decreased  $CF_{ice}$  with  $N_a$  across SSTs, as illustrated in Fig. 5a. The enhanced  $\Delta LWC$  is also consistent with the reduction in  $\Delta R^{LW}$  presented in Fig. 1b.*”



13. L219: “lower SSTs, contributed mostly by a stronger SW response.”: Fig. 1 shows, especially in the colder simulations, quite similar SW and LW components to the CRE.

**Reply:** The sentence was rewritten to better match the data presented: “*We also show that this effect is stronger under lower SSTs, which is consistent with the stronger increase in liquid water path ( $\mathcal{L}$ ) with  $N_a$  under lower SSTs. The ice water path ( $\mathcal{I}$ ) and cloud fraction (CF) responses, on the other hand, are negative and consistent across SSTs.*”

14. L228: I’m not sure this is shown clearly enough to be a conclusion. Cloud morphology, overlap, and anvil coverage may also impact the SW reflection.

**Reply:** Thank you. Following your first comment and comments made by Reviewer #1, we identified the existence of shallow clouds and used a linear decomposition in order to distinguish between cloud coverage and cloud opacity. Using this decomposition, which was also done for the different identified cloud regimes, we arrived at a more reliable conclusions: “*To better understand these trends, we decompose the response of TOA energy gain ( $\Delta R$ ) to different cloud regimes (based on 2D histograms of  $\mathcal{L}$  and  $\mathcal{I}$ ) and to contributions from changes in the cloud opacity (the opacity term) and in cloud occurrence (the shift term) based on a linear decomposition. This decomposition illustrates that most of  $\Delta R$ 's negative trend and its SST-sensitivity is driven by the opacity term, which in turn is driven by the SW part of the spectrum. This trend can be explained by the Twomey effect, i.e, for a given  $\mathcal{L}$  and  $\mathcal{I}$  the clouds become more reflective with a rise in  $N_a$ . The Twomey effect is proportional to the baseline CF, thus becoming stronger under lower SST for which the baseline CF is higher. The shift term, on the other hand, illustrates a compensation between a positive response in the SW and a negative response in the LW, thus producing a small net effect. Furthermore, we decompose  $\Delta R$  and its components per cloud regime, which illustrates that ice and shallow clouds are the main drivers behind the opacity and shift terms trends.*”

15. L245: This paragraph generally nicely explains the limitations of the simulation. I would perhaps also add that the finding that increased  $N_a$  increases precipitation could lead to moderation of  $N_a$  through faster rates of wet deposition, but that here  $N_a$  was prescribed.

**Reply:** Please refer to our answer to general comment 3.

Figures: 1. Fig. 7: Please explain how this is calculated. It is not obvious to me how  $Q_r$  could be held fixed in any given simulation

**Reply:** Please refer to our answer to comment 7.

### Minor comments

1. L74: “vertical pressure velocity” → “clear sky vertical pressure velocity”

**Reply:** Thank you. The line was rewritten as suggested.

2. L81: “and observations to decrease with surface temperature ” → “and observations to decrease in coverage with surface temperature ”

**Reply:** Thank you. The sentence was rewritten: “*While observations, global climate models and high-resolution, convective-permitting models predict an increase in altitude of anvil clouds while maintaining nearly fixed temperatures, they also anticipate a decrease in anvil cloud coverage with rising surface temperatures*”

3. L112: “solar-insulation” → “solar insolation”

**Reply:** Thank you. The line was rewritten as suggested.

4. L115: “is fixed at pre-industrial level (280 ppm)” → “is fixed at the pre-industrial level (280 ppm)”

**Reply:** Thank you. The line was rewritten as suggested.

5. LL118: “The vertical profile of O<sub>3</sub> ’s represents”: I suggest simply O<sub>3</sub> or just “ozone”

**Reply:** Thank you. The sentence was rewritten: “*A fixed ozone profile, representing a typical tropical atmosphere, is used here.*”

6. L141: “the isotherm height” → “freezing level”

**Reply:** Thank you. The line was rewritten as suggested.

7. L160: “reduction in cloud ice at the upper troposphere (Fig. 3f),”: I think you meant 3h.

**Reply:** Thank you. The sentence was rewritten: “*In addition, cloud ice declines with  $N_a$ , consistently across SSTs (Fig. 3h).*”

8. L199: “calculated as the TOA’s LW radiation flux” → “calculated as the TOA’s net LW radiation flux”. Right?

**Reply:** Thank you. The line was rewritten as suggested.

9. L227: “Hence, the liquid water content in clouds” → “Hence, the column liquid water content in clouds”

**Reply:** Thank you. Due to revisions made in the paper as mentioned in our answer to comment 14, this is no longer relevant.

10. L256: “ACI”: Spell out explicitly here please

**Reply:** Thank you. The line was rewritten as suggested.

### Suggestions

The comments in this section are intended to be more suggestive. The authors are welcome to take them into consideration but need not feel obligated to.

1. L80: “Beside increasing in height”: This is the first explicit mention of the prediction that anvils will rise with FAT. If a reader was not familiar with FAT, it could be nice to introduce it in the paragraph beginning at line 67.

**Reply:** The FAT hypothesis is indeed mentioned in line 66.

2. Fig. 4 and 10: Perhaps my personal preference, but I would plot on the y-axis the values rather than the difference with the cleanest run. The point would remain the same as this amounts to a vertical shift. If you choose not to, make this more clear in the captions (“relative to the cleanest run for each SST” → “Values are shown as a difference with the cleanest run for each SST.” or similar)

**Reply:** Thank you. Following this suggestion the captions were rewritten for clarity: “*The values are shown as a difference between the most polluted ( $N_a = 2000 \text{ cm}^{-3}$ ) and the cleanest ( $N_a = 20 \text{ cm}^{-3}$ ) runs for each SST.*” We prefer to present the difference from the cleanest run in order to emphasize the effect of aerosol under different SST rather than the effect of SST.

3. I might add a thin dashed line on all plots that present changes along the  $\Delta\phi = 0$  line where  $\phi$  is the variable being plotted (similar to Fig. 10).

**Reply:** A dashed line marking the zero-value was added in the relevant figures.

4. The font sizes in plots are inconsistent. Assuming these are generated in Python, this could be fixed by setting `figsize` to a constant value in `plt.subplots(figsize=(width, height))` and then setting the font sizes to constant values in `ax.set_ylabel()`, `ax.set_title()` etc.

**Reply:** Thank you. The font in all the figures was set to a constant value as suggested, besides in Fig. 11, where the font was made to be slightly bigger to ensure comfortable reading.

5. L182: Perhaps define  $h_L$  mathematically to make clear this includes latent energy from freezing.

**Reply:** Thank you. We specified that the latent term in  $h_L$  includes latent energy from freezing: “The  $h_L$  tendency equation contains 5 terms: advection (*adv*), radiation (*rad*), latent heating (includes latent heating from freezing), turbulence and large-scale tendency”

6. L220: “pushes warm rain initiation to higher levels of the cloud” → “pushes would-be warm rain initiation to higher levels of the cloud” or something similar. In the colder simulations, these “higher levels” are above the freezing level, so rain does not form as well since the ice crystals “steal” water off the droplets that would become rain. In Fig. 3g, it is only the warmest 2 simulations that show increased rain near the freezing level. This is explained well in the following sentences.

**Reply:** Thank you. We understand the reviewer's point here but believe that this sentence is clearer in its original form since we think “.. would-be warm rain initiation...” might be hard to understand.

7. L253: “allow us to confront our conclusions”: Did you mean confirm?

**Reply:** We meant that we want to check whether our conclusions are correct in a variety of models and microphysical schemes, hence the use of the word “confront” and not “confirm”.

## References

Bony, Sandrine, et al. “Thermodynamic control of anvil cloud amount.” *Proceedings of the National Academy of Sciences*, vol. 113, 2016, 8927--8932.

Choudhury, G., and M. Tesche. “A first global height-resolved cloud condensation nuclei data set derived from spaceborne lidar measurements.” *Earth System Science Data*, vol. 15, 2023, 3747--3760, <https://essd.copernicus.org/articles/15/3747/2023/>.

Sokol, Adam B., et al. "Anvil cloud thinning implies greater climate sensitivity." 2024,

[https://atmos.uw.edu/~abs66/docs/Sokol\\_et\\_al\\_2024\\_preprint.pdf](https://atmos.uw.edu/~abs66/docs/Sokol_et_al_2024_preprint.pdf).

Twomey, Sean. "The influence of pollution on the shortwave albedo of clouds." *Journal of the atmospheric sciences*, vol. 34, 1977, 1149--1152.

Wing, Allison A., et al. "Clouds and convective self-aggregation in a multimodel ensemble of radiative-convective equilibrium simulations." *Journal of advances in modeling earth systems*, vol. 12, 2020.